Cold Regions Science and Technology 124 (2016) 118–126

Contents lists available at ScienceDirect

Cold Regions Science and Technology

journal homepage: www.elsevier.com/locate/coldregions

Frost depth prediction for seasonal freezing area in Eastern Turkey

Muge Elif Orakoglu [a,b], Jiankun Liu [a,*], Erol Tutumluer [c]

[a] School of Civil Engineering, Beijing Jiaotong University, Beijing 100044, China
[b] Technical Education Faculty, Construction Department, Firat University, Elazig 23000, Turkey
[c] Civil and Environmental Engineering Department, University of Illinois at Urbana-Champaign, Urbana, IL, United States

ARTICLE INFO

Article history:
Received 27 November 2014
Received in revised form 29 March 2015
Accepted 31 December 2015
Available online 30 January 2016

Keywords:
Frost-related problems
Frost heave
Subgrade
Cold regions in Turkey

ABSTRACT

This paper presents the results of an investigation relative to the prediction of frost depths of seasonal freezing area in eastern Turkey. The Stefan equation and a modified Berggren equation are compared and utilized, and the computed results are compared with actual observed data. Also, the different harmful effects of freezing–thawing on highways in eastern Turkey are elucidated, supplemented with case studies. Based on this, the coldest areas are defined and a freezing depth contour map with the region's transportation network is produced. Some recommendations for the design and maintenance of subgrades in cold regions are provided.

1. Introduction

Seasonal frozen ground is widely distributed in eastern Turkey. Understanding the heat and mass transfer processes in these areas is highly important for solving civil engineering and infrastructure-related problems. Previous studies have shown that mechanical and physical properties of soil can be changed during the freezing–thawing process, which may negatively affect the subgrade function (Zaimoglu, 2010; Aubert and Gasc Barbier, 2012; Oztas and Fayetorbay, 2003; Cui et al., 2014; Kalkan, 2009; Graham and Au, 1985; Yarbasi et al., 2007; Altun et al., 2009; Angin et al., 2013; Olgun, 2013; Simonsen and Isacsson, 2001). Materials incorporating fibers, conventional elements, enzymes, and polymeric resins can be used for mitigation of these negative effects on soils subjected to freezing–thawing.

Seasonal soil freezing and thawing are significantly influenced by soil water conditions, soil thermal properties, snow cover rate, and local climatic conditions (precipitation, temperature changes, and solar radiation) in cold regions. Xiang et al. (2013) revealed the effects of climate variation on freezing and thawing processes. Li et al. (2012) simulated soil water and heat dynamics during winter periods with a 1-D Simultaneous Heat and Water (SHAW) model using soil temperature and soil water content in seasonal frozen soil areas. Isard and Schaetzl (1995) developed a physically-based computer model in order to examine regional trends in soil temperature and freezing and to compare these trends to patterns of snow thickness and air temperature. Flerchinger (2013) discussed the effects of soil freezing on moisture movement, frost heave, infiltration, erodibility, aggregate stability, and solute movement, and explained these with some examples illustrating the influence of soil texture on soil freezing dynamics and aggregate stability.

Numerical and experimental methods are commonly utilized to determine frost penetration depths and freezing and thawing times. Iwataa et al. (2012) measured frost penetration depths in the Tokachi District in Japan using the method of frost tubes filled with methylene blue solution. Miller et al. (2012) estimated frost and thawing times at many test sites using a freeze–thaw index model. Hong et al. (2011) described the empirical equations for frost penetration depths in South Korea based on field measurements over the last two decades, and Cleland et al. (1987) assessed the accuracy of numerical methods used in the prediction of freezing and thawing times using a comprehensive set of freezing and thawing data for both regular and irregular multi-dimensional shapes. Moreover, Bianchini and Gonzalez (2012) reported that the solution of the heat equation applied to a 1-D homogeneous and isotropic layer, which is currently implemented in the Pavement Transportation Computer Assisted Structural Engineering (PCASE) software, which incorporates a more accurate numerical solution of the modified Berggren (hereafter, ModBerg) equation. The Massachusetts Institute of Technology Department of Civil and Sanitary Engineering, Soil Engineering Division (MIT, 1957) presented the results of an investigation into the prediction of the depth of frost penetration in multi-layer soil profiles. An adaptation of the ModBerg equation was presented and compared with “exact” solutions for the depth of freezing as determined by the hydraulic analog computer developed under the contract. Johnston (1982) used the ModBerg

* Corresponding author. Tel./fax: +86 10 5168409.
E-mail addresses: mugeorakoglu@gmail.com (M.E. Orakoglu), jkliu@bjtu.edu.cn (J. Liu), tutumlue@illinois.edu (E. Tutumluer).

http://dx.doi.org/10.1016/j.coldregions.2015.12.012
0165-232X/

Table 1
Snow pack in Turkey.

Regions	Snow-pack (m)	Regions	Snow-pack (m)
The Central Anatolian		The Black Sea	
Ilgaz	0.15	*Gerede*	0.15
Yildiztepe	0.13	*Bayburt*	0.11
Eastern Turkey		The Marmara	
Palandoken	0.30	*Uludag*	0.14
Sarikamis	0.26		
Mus	0.28	Northern Mediterranean	
Agri	0.14	*Davraz*	0.20

Table 2
The mean monthly temperatures of eastern Turkey.

The mean monthly temperatures, v_o (°C)					
	January	*February*	*March*	*November*	*December*
A soil profile: *Erzurum, Kars, Agri*	−15.38	−13.63	−6.88	−5.96	−9.13
B soil profile: *Igdir, Van, Bingol*	−8.35	−7.22	−1.03	1.62	−4.82
C soil profile: *Bitlis, Mus, Erzincan, Tunceli*	−7.16	−5.87	0.27	2.06	−4.02
D soil profile: *Elazig, Malatya, Hakkari*	−5.80	−5.50	0.35	2.90	−1.90

Table 3
The air freezing and surface freezing indices of eastern Turkey based on mean monthly temperatures.

	Freezing index I_{af} (°C-days)	Actual frost depths (m)	Surface freezing index I_{sf} (°C-days)
A soil profile	1900	1.40–1.60	1710
B soil profile	1400	1.20–1.39	1260
C soil profile	650	0.80–0.99	585
D soil profile	375	0.69–0.79	337.5

equation to predict the thickness of fill required for the conditions at an Inuvik site in Canada because it was apparent that a substantial fill would be needed to prevent thawing of the underlying frozen ground.

Many researchers have studied permafrost-related problems on railways and highways. He and Jin (2010) reviewed the history of permafrost and environmental problems of oil pipelines in cold regions. Tan et al. (2011) determined that the application of insulation material near the exit of the Galongla Tunnel (in Tibet) could effectively prevent freezing–thawing damages to the lining and surrounding rock. Simonsen and Isacsson (1999) reviewed the problems associated with soil weakening and bearing capacity of pavement during thaw processes. Wen et al. (2010) evaluated a probabilistic model for the replacement thickness of in-cuts in roadbeds in permafrost regions, and designed the in-cuts for the Qinghai–Tibetan Railway roadbed to protect the permafrost under the replacement layer. Shoop et al. (2002) assessed various stabilization techniques and their recommended applications based on expected soil frost conditions and traffic requirements. Because many civil engineering problems are related to frost heave and frost-susceptible soils in cold regions, Kamiloglu et al. (2012); Zhao et al. (2012), and Isik et al. (2013) examined some factors affecting frost heave under freezing–thawing cycles. Bronfenbrener (2009) developed a new model to predict the freezing process in porous media.

Freezing depth is essential to engineering design in cold region, but this was not studied enough for cold part of Turkey. The goal of this paper is to evaluate the characteristics of seasonal ground freezing in eastern Turkey, summarize the related engineering problems in transportation infrastructures, and provide some recommendations for the design and maintenance of subgrades in cold regions.

2. Climatic conditions and transportation lines in Eastern Turkey

The definition of a "cold region" requires both climatological and geographical descriptions. For example, climatologists consider the isotherm for 0 °C mean temperature during the coldest month of the year as defining the southern limit of the cold regions in the Northern Hemisphere. Seasonal and permanently frozen grounds, as characteristics of cold regions, have drawn new interest from many geotechnical engineers (Andersland and Branko, 2004).

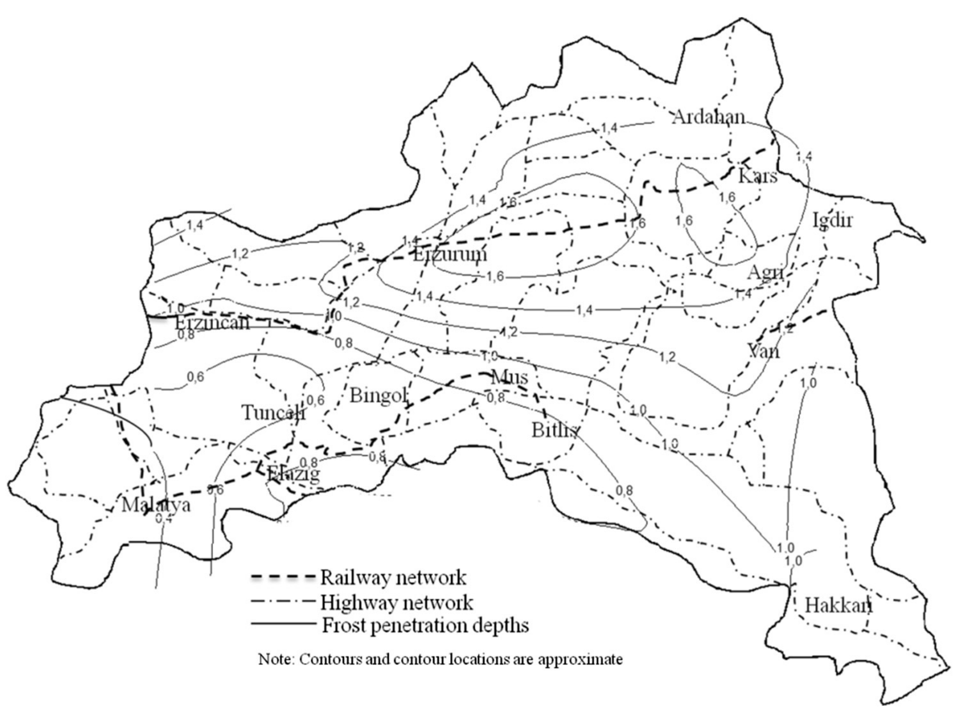

Fig. 1. Predicted frost penetration depths contour map and the main transportation networks in eastern Turkey.

Table 4
n-Factor values of some surfaces.

Surface	Freezing, n_f	Thawing, n_t
Sand and gravel	0.9	2.00
Vegetation and 6-cm soil stripped, mineral soil surface	0.25	0.73
Gravel	0.6–1.0	1.3–2
(Probable range, northern conditions)	(0.9–0.95)	–
Trees and brush cleared moss over peat soil	0.25 (under snow)	0.73
Spruce trees, brush, moss over peat soil	0.29 (under snow)	0.37
Turf	0.5	1.0

From Andersland and Branko (2004).

Table 5
Summary of assumed soil properties.

Region and soil profile	Assumed soil properties				
	w (%)	γ_d (g/cm^3)	c (MJ/m^3 °C)	k (W/m °C)	L (MJ/m^3)
Asphalt concrete (250 mm)	21.1	2.2	1.54	2.09	0
Aggregate base (500 mm)	14	1.8	1.76	1.94	84.09
Subgrade	16	1.75	1.86	2.2	144.16

w, optimum moisture content; γ_d, *dry density*; c, heat capacity; k, thermal conductivity; L, latent heat.

Eastern Turkey is located at the latitudes between 37°36′ N and 41°07′N and at the longitudes between 38°28′E and 44°08′E, and covers a territory of about 171,061 km^2. Given the continental cold climate with severe winters and heavy rainfall in eastern Turkey, a great majority of the region is subjected to damaging frost effects. In many recent years, the mean annual temperature in eastern Turkey has reached unprecedented low extremes. The average annual temperature of eastern Turkey in winter fluctuates between −18.0 °C and +7 °C. This region has a semi-dry, less humid climate, where the freezing period is from November to March of the following year. The eastern part receives 2200 mm of precipitation annually and is the only region of Turkey that receives rainfall throughout the year. In the eastern part of that area, snow lies on the ground for approximately 120 days of the year (Sensoy et al., 2008). The effect of snow pack plays a major role on the ground thermal regime. In cold regions, the thicknesses of the soil layers hinder snowmelt infiltration, which influences the hydrological cycles and thus increases runoff of spring snowmelt water (Iwataa et al., 2011). Table 1 shows snowmelt infiltration in Turkey. In the western part of the area, which is characterized by warm air temperature, a frozen layer does not form under the snow pack and most of the snowmelt water infiltrates into the ground, which does not occur in the eastern part.

The differences in temperature and the geographic features have strongly influenced the design of the transportation lines in eastern Turkey. There are approximately 10,492 km of roadways in eastern Turkey. The roadways are classified by a four-tier system: motorways (multi-lane, access-controlled highways), state roads, provincial roads, and rural roads (RTMT, 2011). The railway lines in eastern Turkey have progressed rapidly since 1950, and many more high-speed railway lines in the region have been planned or are under construction. However, the geographic features, hydrogeological conditions, natural structures and frost-susceptible soil conditions in eastern Turkey have delayed construction of some of these high-speed railway lines.

Ground freezing and thawing problems are common in eastern Turkey and are affected by the large differences in mean annual temperature described earlier. During climate changes, there is a circulation between the water content in the unfrozen regions and the freezing fronts.

The volume of soil will increase by 9% when the water in the soil becomes ice, and the soil mass forms unequal frost heaves (Lautala et al., 2012). Therefore, before any engineered construction, a frost heave sensitivity analysis and assessment of the soil layers should be conducted. The frost penetration depths for the design of transportation lines in eastern Turkey have been determined by the Republic of Turkey

Table 6
Results of the predicted values for the Stefan and the ModBerg equations on a multilayer soil.

		Variations of Frost Depths									
A soil profile	v_o (°C)	**−15.38 °C**		**−13.63 °C**		**−6.88 °C**		**−5.97 °C**		**−9.13 °C**	
		X_{STE}	X_{MOD}	X_{STE}	X_{MOD}	X_{STE}	X_{MOD}	X_{STE}	X_{MOD}	X_{STE}	X_{MOD}
	AFD:1.40	1.949	1.403	1.893	1.401	1.707	1.400	1.647	1.400	1.774	1.401
	AFD:1.45	2.077	1.454	2.05	1.455	1.993	1.455	1.839	1.453	1.912	1.453
	AFD:1.50	2.15	1.505	2.114	1.501	2.059	1.5	1.904	1.504	1.976	1.502
	AFD:1.55	2.215	1.550	2.18	1.553	2.13	1.556	1.968	1.554	2.04	1.551
	AFD:1.60	2.28	1.601	2.26	1.604	2.19	1.603	2.031	1.605	2.11	1.606
B soil profile	v_o (°C)	**−8.35 °C**		**−7.22 °C**		**−1.03 °C**		**1.62 °C**		**−4.82 °C**	
		X_{STE}	X_{MOD}	X_{STE}	X_{MOD}	X_{STE}	X_{MOD}	X_{STE}	X_{MOD}	X_{STE}	X_{MOD}
	AFD:1.20	1.564	1.205	1.464	1.201	1.281	1.204	1.299	1.208	1.381	1.202
	AFD:1.25	1.627	1.253	1.437	1.250	1.335	1.255	1.345	1.251	1.436	1.250
	AFD:1.30	1.693	1.304	1.573	1.305	1.391	1.307	1.400	1.302	1.501	1.306
	AFD:1.35	1.756	1.352	1.556	1.353	1.437	1.351	1.455	1.353	1.552	1.350
	AFD:1.39	1.811	1.394	1.600	1.393	1.481	1.392	1.499	1.394	1.637	1.391
C soil profile	v_o (°C)	**−7.16 °C**		**−5.87 °C**		**0.27 °C**		**2.06 °C**		**−4.02 °C**	
		X_{STE}	X_{MOD}	X_{STE}	X_{MOD}	X_{STE}	X_{MOD}	X_{STE}	X_{MOD}	X_{STE}	X_{MOD}
	AFD:0.80	1.016	0.802	0.97	0.805	0.869	0.808	0.924	0.804	0.897	0.807
	AFD:0.85	1.079	0.853	1.025	0.850	0.915	0.851	0.979	0.852	0.951	0.855
	AFD:0.90	1.144	0.904	1.089	0.903	0.97	0.902	1.043	0.907	1.006	0.905
	AFD:0.95	1.207	0.954	1.153	0.957	1.025	0.953	1.097	0.954	1.057	0.951
	AFD:0.99	1.254	0.991	1.198	0.995	1.069	0.994	1.143	0.995	1.107	0.996
D soil profile	v_o (°C)	**−5.80 °C**		**−5.50 °C**		**0.35 °C**		**2.90 °C**		**−1.90 °C**	
		X_{STE}	X_{MOD}	X_{STE}	X_{MOD}	X_{STE}	X_{MOD}	X_{STE}	X_{MOD}	X_{STE}	X_{MOD}
	AFD:0.69	0.878	0.694	0.868	0.694	0.731	0.695	0.832	0.691	0.749	0.697
	AFD:0.70	0.887	0.701	0.878	0.702	0.741	0.704	0.851	0.706	0.759	0.706
	AFD:0.75	0.952	0.751	0.94	0.753	0.795	0.755	0.905	0.751	0.813	0.756
	AFD:0.77	0.979	0.773	0.97	0.775	0.815	0.774	0.932	0.774	0.832	0.774
	AFD:0.79	1.007	0.795	0.996	0.796	0.832	0.791	0.96	0.797	0.851	0.791

AFD, Actual frost depths suggested by Republic of Turkey General Directorate of Highways (m); X_{STE}, frost depth according to the Stefan equation; X_{MOD}, frost depths according to the ModBerg equation.

Directorate General for Highways (Saglik and Gungor, 2000). Fig. 1 depicts the frost penetration depth contour map and the main transportation networks in eastern Turkey.

3. Characterization of the cold region and transportation-related soil problems in Eastern Turkey

The ground temperature factor is significant in the design of transportation networks throughout the world, especially in cold regions. It leads to many problems which cause serious damage to transportation lines and economic loss. Turkey is challenged by having several different climatic types, frost-thaw indices and frost depths. Of these regions, the Eastern Anatolia region has the coldest and the harshest weather conditions.

3.1. Numerical modeling

The degree-day concept is commonly used in describing the intensity of air temperatures. During a year, the air freezing index (I_{af}) is the number of negative (T < 0 °C) degree-days between the highest and lowest points on a curve of cumulative degree-days versus time, whereas the air thawing index (I_{at}) is the number of degree-days between the minimum in the spring and the maximum in the next autumn. Any spring or autumn month that includes a seasonal maximum or minimum is called a changeover month. For these changeover months, an equation was proposed by D.W. Boyd;

$$\left(Y^2 - NTY = N^2 k^2\right) \tag{1}$$

where Y is a variable indicating degree-days, k is a constant, and T is the average temperature (°C) in a month of N days (Andersland and Branko, 2004).

A seasonal index is defined as the seasonally integrated temperature, which is approximately equal to the sum of daily mean temperatures for the duration of the season. For example, the thawing index developed by Klene et al. (2001) is:

$$I_{TS} = \int_0^{\theta_s} (T_S - T_F)dt \approx \sum_0^{\theta_S} \overline{T_S} \tag{2}$$

where T_F is the temperature of the freezing point (0 °C); T_S is the surface temperature (°C), θ_S is the duration of the thawing season, days; and $\overline{T_s}$ is the daily mean surface temperature.

The seasonal freezing and thawing depths are a result of climate change. Generally, the air thawing (I_{at}) and air freezing (I_{af}) indices are used to elucidate seasonal freezing and thawing problems. The surface parameters, including snow pack, vegetation, and ground thermal

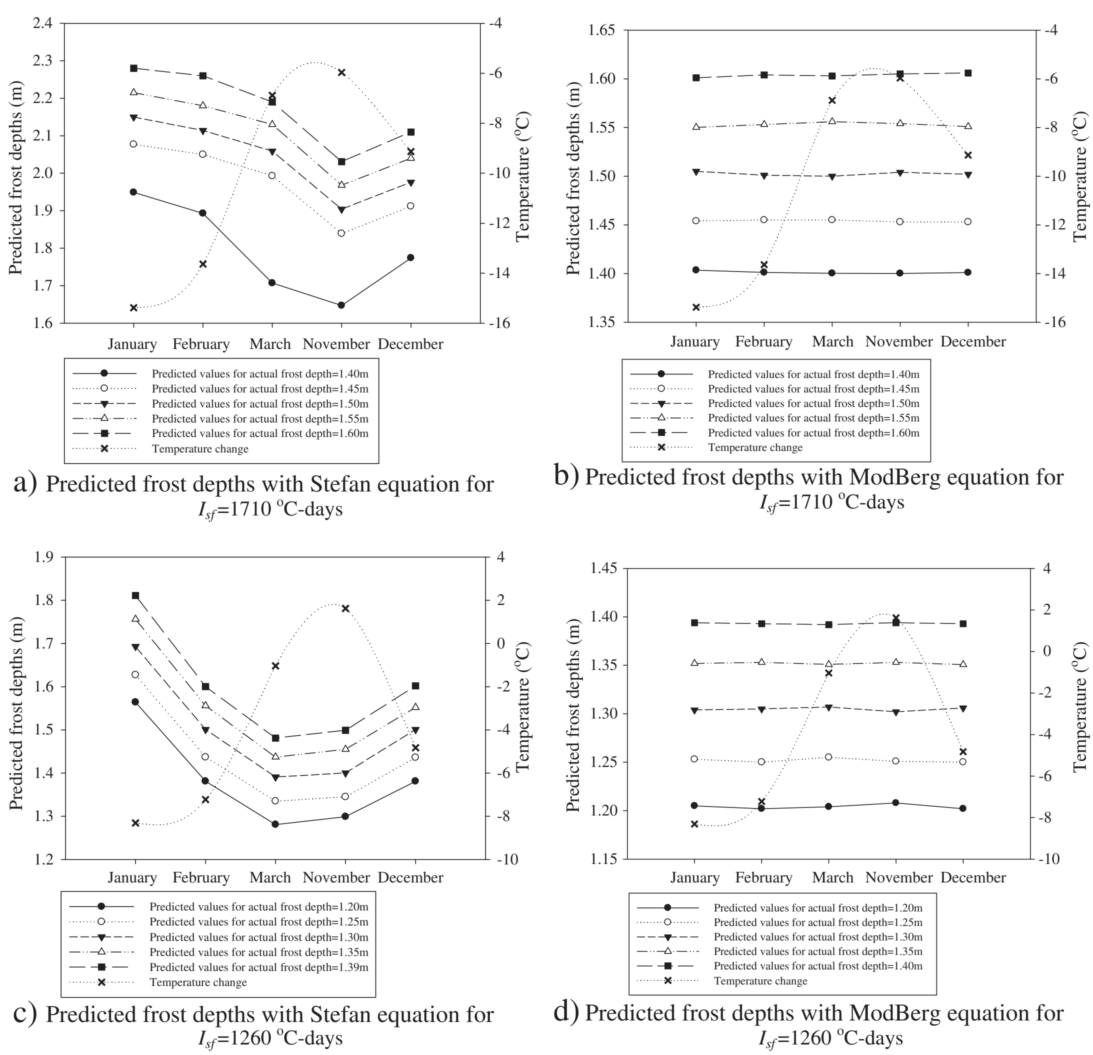

Fig. 2. Comparison of the Stefan equation and the ModBerg equation results.

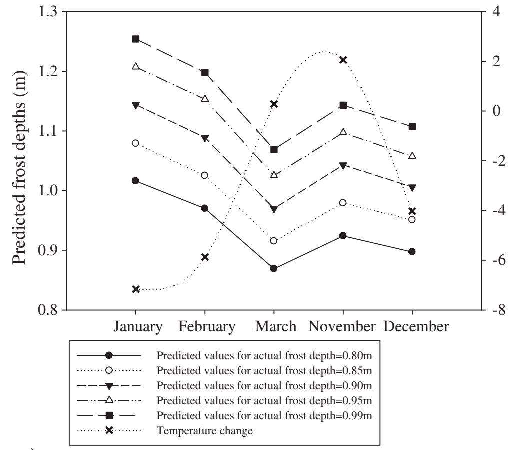

e) Predicted frost depths with Stefan equation for I_{sf}=585°C-days

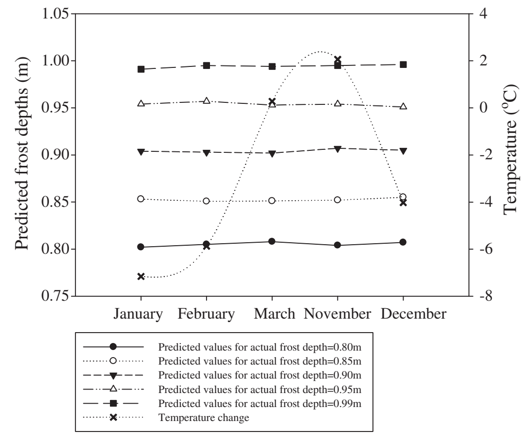

f) Predicted frost depths with ModBerg equation for I_{sf}=585°C-days

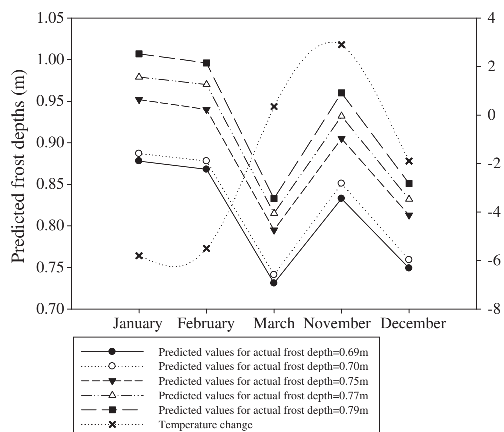

g) Predicted frost depths with Stefan equation for I_{sf}=375°C-days

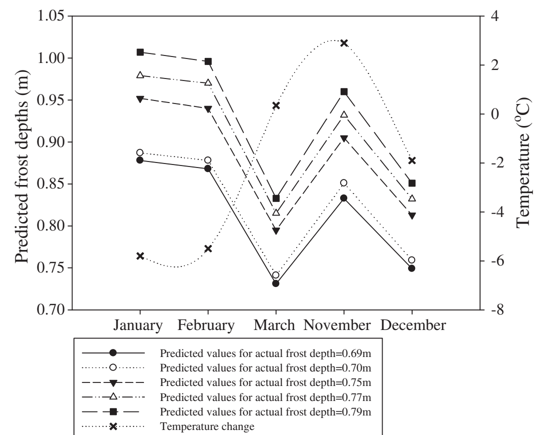

h) Predicted frost depths with ModBerg equation for I_{sf}=375°C-days

Fig. 2 (*continued*).

properties, are determined by using surface *n*-factors that are based on the surface freezing index (I_{sf}) and the air freezing (I_{af}) index:

$$n_f = \frac{I_{sf}}{I_{af}}. \tag{3}$$

Many researchers have proposed various surface *n*-factors to be utilized for different surface layers (Carlson, 1952; Klene et al., 2001; Jorgenson and Kreigh, 1988).

In this paper, the actual values of the frost depths and the air freezing indices suggested by the Republic of Turkey General Directorate of Highways (Saglik and Gungor, 2000) in eastern Turkey are utilized and classified as four regions according to the surface freezing index (I_{sf}) to predict the frost depths using Stefan and ModBerg equations. Tables 2 and 3 show the mean monthly temperatures (v_o) in the coldest season, the air freezing indices, calculations of the surface freezing indices and the actual frost depths in eastern Turkey. Also shown are the mean monthly air temperature data which were acquired by the Turkish State Meteorological Service (TSMS) over the period of 1960–2012. An uniform coarse-grained soil subgrade with 16% water content were examined, with the different surface freezing indices by using the surface n-factors presented by McRoberts (1974), Luardini (1978 and 1985) and Department of Army (1966) (Table 4).

Frost depths in cold regions are important parameters affecting snowmelt infiltration ratios, which can damage subgrade layers. The frost depths are related to climatic conditions, subgrade thermal properties, energy balance, and snow pack. Many methods for predicting the depths of freeze and thaw in soils are described in the literature (e.g., Jumikis, 1977; Iwataa et al., 2011; Coskun et al., 2009, Haciefendioglu et al., 2013).

Approximate solutions based on equations for homogeneous soil and semi-empirical computation techniques are generally used for multi-layer soils to calculate frost depths. In this context, we used the Stefan and the ModBerg to predict frost depths of multilayer soils in eastern Turkey. We assumed that the thermal properties of the soils and boundary temperature conditions were known and that the initial temperature of soil was uniform and then suddenly changed to a temperature below the freezing point.

The Stefan solution was modified for use with soils and is one of the most basic and commonly used methods for predicting active-layer thickness, because Stefan's first equation neglected the effects of volumetric heat capacity, tending to overestimate frost depth (Schimek, 2011):

$$X = \sqrt{\frac{2k_{fro}\int v_s dt}{L}} \tag{4}$$

where X is the frost depth (ft), k_{fro} is the thermal conductivity of frozen soil (Btu/(h ft °F), v_s is the effective surface temperature (°F days), and L is the latent heat (Btu/ft^3).

a) Stripping of bitumen layer (Karayolu Haber, 2013)

b) Cuts in road due to water (Beyaz Gazete, 2013)

c) Cuts in road due to water, (Haberler, 2014)

Fig. 3. a) Stripping of bitumen layer (Karayolu Haber, 2013). b) Cuts in road due to water (Beyaz Gazete, 2013). c) Cuts in road due to water (Haberler, 2014).

In the Stefan solution, the partial freezing index required to freeze any layer "n" (F_n) and the total freezing index (F) for any period can be determined:

$$F_n = \frac{L_n d_n}{24}\left(\frac{d_1}{k_1} + \frac{d_2}{k_2} + \ldots + \frac{d_n}{2k_n}\right)$$
$$F_n = \frac{U_n}{24}\left(R_1 + R_2 + \ldots + \frac{R_n}{2}\right) \tag{5}$$

$$F = \frac{U_1}{24}\left(\frac{R_1}{2}\right) + \frac{U_1}{24}\left(R_1 + \frac{R_2}{2}\right) + \ldots + \frac{U_m}{24}\left(R_1 + R_2 + \ldots + \frac{R_m}{2}\right) \tag{6}$$

where $U_n = L_n d_n$ is the latent heat (L_n) removed when freezing the n^{th} layer of thickness d_n; and $R_n = d_n/k_n$ is the thermal resistance for thermal conductivity k_n of thickness d_n.

Moreover, the values of effective L/k for the frozen zone were calculated by substituting the total freezing indexes:

$$\left(\frac{L}{k}\right)_{eff.} = \frac{2}{X^2}\left[\begin{array}{l} \frac{d_1}{k_1}\left(\frac{L_1 d_1}{2} + L_2 d_2 + \ldots + L_m d_m\right) \\ + \frac{d_2}{k_2}\left(\frac{L_2 d_2}{2} + L_3 d_3 + \ldots + L_m d_m\right) \\ + \ldots + \frac{d_m}{k_m}\left(\frac{L_m d_m}{2}\right) \end{array}\right]. \tag{7}$$

On the other hand, the net heat flux at the frost line states the latent heat released by the soil moisture, as it freezes at depth d_X in time d_t, equals the rate at which heat is conducted to the ground surface. Bianchini and Gonzalez (2012) stated that the ModBerg equation is derived from starting integrated the Fourier's law and to quantify heat transferred a homogenous soil profile. The temperatures at the upper and lower surfaces, T_1 and T_2 ($T_1 < T_2$) for a soil layer of thickness X were utilized. The ModBerg model's assumption is that the temperature differential $T_1 - T_2$ is constant and is equal to the average of the differences between the annual mean temperature and the freezing temperature (32 °F). In Eq. (8), X represents the depth at which the material will reach the freezing temperature. The depth X of frost-depth penetration in multi-layered soil systems that utilize a correction coefficient λ to the depth of frost penetration, based on the ModBerg equation, is extracted as:

$$X = \lambda\sqrt{\frac{2kv_s t}{L}} \tag{8}$$

where X is the depth of frost penetration (ft), λ is the correction coefficient which considers the effect of temperature changes in the soil mass (i.e., a fudge factor), k is thermal conductivity (average of frozen and unfrozen soil) (Btu/(hr ft °F), and L is the volumetric latent heat (Btu/ft^3).

Also, a step change in surface temperature is expressed by the surface temperature changing suddenly from v_o degrees above freezing to v_s degrees below freezing where it remains constant. We assumed that weighted variables of volumetric heat (C) and latent heat (L) within the frost depths X for which the time is desired as the following:

$$C_{wt} = \frac{c_1 d_1 + c_2 d_2 + \ldots + c_m d_m}{X} \tag{9}$$

$$L_{wt} = \frac{L_1 d_1 + L_2 d_2 + \ldots + L_m d_m}{X}. \tag{10}$$

The summary of results for the Stefan equation and the ModBerg equation for the multilayer soil profile is given in Table 4. In eastern Turkey, the actual frost depths are seen to be restricted to between 0.6 m and 1.6 m (Fig. 1 and Tables 5 and 6). We predicted the frost depths using the Stefan and the ModBerg solutions for ranges of these actual values and different v_o temperatures. Also, the actual values of the correction coefficients (λ, λ_{MBD}) were defined to compare the results of Eqs. (11) and (12):

$$\lambda = \frac{X}{X_S} \tag{11}$$

$$\lambda_{MBD} = \frac{X_{MB}}{X_S} \tag{12}$$

where X is the actual frost depths at any time for any freezing index, X_s is the frost depth at the same time for the same freezing index according to the Stefan equation, and X_{MB} is the frost depth according to the Modified Berggren equation.

Fig. 2 shows a comparison of predicted frost depths and actual frost depths for eastern Turkey.

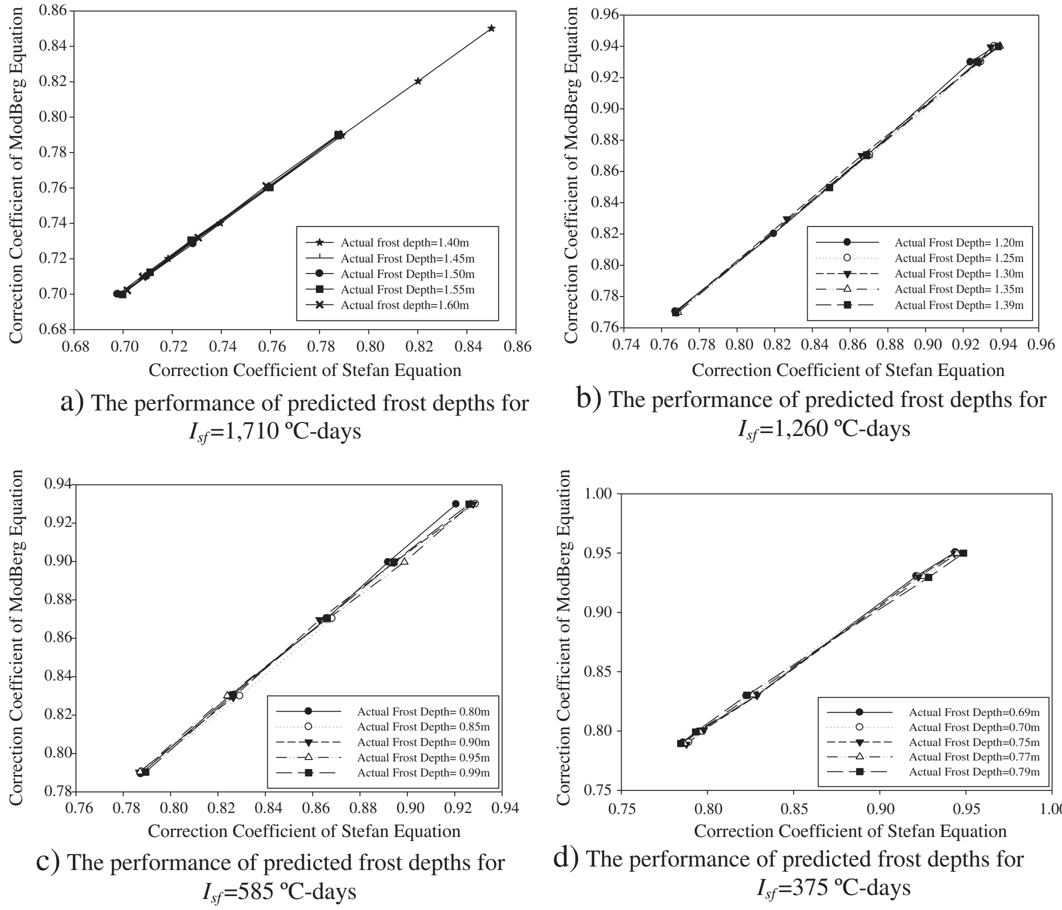

Fig. 4. a) The predicted frost depths for Isf = 1710 °C-days. b) The predicted frost depths for Isf = 1260 °C-days. c) The predicted frost depths for Isf = 585 °C-days. d) The predicted frost depths for Isf = 375 °C-days.

3.2. The main transportation-related soil problems resulting from freezing–thawing in Eastern Turkey

In the eastern region of Turkey, road construction and earthwork applications are usually constructed in freeze–thaw environments. If a highway structure develops fatigue cracks, new cracks produced by the effects of traffic loads will occur. Moreover, the cracks caused by different settlements during freeze–thaw-related road widening may appear between a new asphalt layer and the old asphalt layer. Also, shear forces occur under heavy traffic loads, and cracking and spalling take place on the asphalt layers that are exposed to these shear forces (Simonsen and Isacsson, 1999; Qi et al., 2012). Under changing climatic conditions, frost heaves are seen on cracked and spalled surfaces during the freezing period, and spring thawing will strongly affect these surfaces (Saltan et al., 2012; Maccaferri Environmental Technology Engineering, 2012; Karaca et al., 2011).

The thaw consolidation problems in eastern Turkey have arisen from excess pore pressure, void ratio changes, unit weight changes in soils, and water content changes. There is a linear relationship between excess pore pressure and the increment of temperature. The different effects of the thaw-weakening problems in eastern Turkey on highways, which are here supplemented with case studies, are given in Fig. 3a–c.

3.2.1. Mus–Bingol Highway

The thawing effects may cause removal of bitumen and longitudinal cracking on surface layers of asphalt roads, and vibrations produced by vehicles may enlarge these cracks. Moreover, at this location these highway damages allow water to penetrate down through the pavement, causing saturation of the unbound base (Fig. 3a). This can lead to permanent deformations and further cracking. The aggregate bituminous layer in the pavement can fracture due to the water and ice.

3.2.2. Sirnak–Beytussebap Road–Sirnak Road

The thawing condition of this road (Fig. 3b,c) is getting worse during the passage of time. During the winter when the soil layer is exposed to freezing, ice granules can be seen in subgrades which have the greatest water potential and the pores have the largest frost points. Thus, the stiffness of the unbound layer generally will be increased (Xiang et al., 2013; Johansson, 2009). In the bituminous layer, the stiffness increases with the decreasing of temperature, and the overall bearing capacity of the coating layer increases. However, during the spring thawing, the bearing capacity can be drastically reduced because thawing ice can enter into the pavement structure. Remarkable settlement may appear if the thawing structure exposes the burden. The snow pack rate and the frozen depth of the subgrade layer can extend the thaw-weakening period and can reduce the bearing capacity. The shear strength of the soil also decreases during thawing.

4. Discussion and recommendations

Using the ModBerg equation and the Stefan equation on multi-layer soil profiles to estimate frost depths will provide a good correlation in eastern Turkey. As shown in Fig. 2a–h, the ModBerg equation yields good, exact results for the prediction of frost depths in eastern Turkey because the correction coefficients (λ and λ_{MBD}) have affined. Fig. 4a–d shows the results of λ and λ_{MBD} applied in predicted frost depths with Stefan and ModBerg equations as a function of temperature and the surface freezing index (I_{sf}). For typical freezing in the A soil profile with an I_{sf} of 1710 °C-days, the frost depth will be limited to 1.4002 m and 1.606 m based on the ModBerg, and between 1.647 m and 2.280 m based on the Stefan equation at different temperatures. This is a significantly different from the seasonal surface freezing index, with a frost depth effect that will be relatively greater as the surface index declines. Furthermore, when λ equals λ_{MBD}, the ModBerg equations yield exact results.

The results demonstrate that the validity of the predicted frost depths for the ModBerg equation is good, although multi-layer soil profiles have boundary conditions. The Stefan equation, however, gives overly high prediction values, which are related to the thermal properties of the soil, particularly the thermal conductivity, and in determining the surface temperature from air temperature and micro-meteorological data. Therefore, it is believed that future research related to the prediction of the frost depths should utilize selected actual values, such as the thermal conductivity, the surface temperatures, the air freezing index, and the correction coefficients suggested by this paper.

It should be noted that the lack of drainage under and alongside highways in eastern Turkey exacerbates the thawing problems and causes premature failure of roads. Proper drainage system should be provided in this region at the predicted frost depths.

5. Conclusions

The prediction of frost depths in eastern Turkey using the Stefan equation and the modified Berggren (ModBerg) equation based on actual values over the last 50 years and the different harmful effects of freezing–thawing on roadways in the region are described in this study. A contour map showing actual frost depths and the highways and railways in eastern Turkey is presented. The regional conditions, including temperature change data, frost-thaw indices, and snowfall and snow pack amounts, were factored into our analytic procedures and boundary conditions were determined to predict frost depths with Stefan and ModBerg equations on a multi-layered soil. From these analyses, we found that the results of the ModBerg equation predict frost depths better than the Stefan equation results, assuming that the initial temperature of the soil was uniform and then suddenly changed to a temperature below the freezing point. Also, the predicted variation of the frost depths fit well with that of the upper boundary conditions. These results can therefore be used in follow-up correction coefficient estimations to predict the frost depths for multi-layered soils in frost-affected areas in eastern Turkey. It is expected that these predicted results for frost depths will be usefully incorporated into the design of highways and railways in eastern Turkey, and for developing treatment methods for freeze–thaw related problems.

Acknowledgments

This work was supported by the National Natural Science Foundation of China (Grant No. 41171064 and 51378057) and the National Basic Research Program of China (973 Program, Grant No. 2012CB026104), and Foundation of the State Key Laboratory of Frozen Soil Engineering (05SS011101 SKLFSE201401).

References

Altun, S., Sezer, A., Erol, A., 2009. The effects of additives and curing conditions on the mechanical behavior of a silty soil. Cold Reg. Sci. Technol. 56, 135–140.

Andersland, O.B., Branko, L., 2004. Frozen Ground Engineering. second ed. NJ. John Wiley & Sons, Inc., Hoboken.

Angin, I., Aksakal, E.L., Oztas, T., Hanay, A., 2013. Effects of municipal solid waste compost (MSWC) application on certain physical properties of soils subjected to freeze–thaw. Soil Tillage Res. 130, 58–61.

Jumikis, A.R., 1977. Thermal Geotechnics. Rutgers University Press, New Brunswick, NJ.

Aubert, J.E., Gasc Barbier, M., 2012. Hardening of clayey soil blocks during freezing and thawing cycles. Appl. Clay Sci. 65-66, 1–5.

Bianchini, A., Gonzalez, C.R., 2012. Pavement-transportation computer assisted structural engineering (PCASE) implementation of the modified Berggren (ModBerg) Equation for computing the frost penetration depth within pavement structures. Final Report. Geotechnical and Structures Laboratory, U.S. Army Engineering Research and Development Center, Vicksburg, MS.

Bronfenbrener, L., 2009. The modelling of the freezing process in fine-grained porous media: application to the frost heave estimation. Cold Reg. Sci. Technol. 56 (2–3), 120–134.

Carlson, H., 1952. Calculation of depth of thaw in frozen ground. Frost Action in Soils: A Symposium.Highway Research Board Special Report 2. National Research Council, Washington, DC, pp. 192–223

Cleland, D.J., Cleland, A.C., Earle, R.L., Byrne, S.J., 1987. Prediction of freezing and thawing times for multi-dimensional shapes by numerical methods. Int. J. Refrig. 10 (1), 32–39.

Coskun, S., Unlu, K., Yamankaradeniz, N., Pulat, E., 2009. Experimental study of horizontal ground source heat pump performance for mild climate in Turkey. Energy 34, 1284–1295.

Cui, Z.D., He, P.P., Yang, W.H., 2014. Mechanical properties of a silty clay subjected to freezing–thawing. Cold Reg. Sci. Technol. 98, 26–34.

Department of the Army, 1966. Arctic and Subarctic Construction: Calculation Methods for Determination of depths of freeze and thaw in soils. Technical Manual TM 5-852-6. U.S. Government Printing Office, Washington, D.C.

Flerchinger, G.N., 2013. Heat and water relations during freezing and thawing, freeze–thaw impacts on infiltration, freeze–thaw impacts on aggregate stability and factors affecting the impact. Reference Module in Earth Systems and Environmental Sciences. Elsevier (North Holland Publishing Co., Amsterdam.

Beyaz Gazete, 2013. http://www.beyazgazete.com/haber/2013/2/27/vatandaslardan-bozuk-yol-tepkisi-1685616.html Jan. 21, 2014.

Graham, J., Au, V., 1985. Effects of freeze–thaw and softening on a natural clay at low stresses. Can. Geotech. J. 22, 69–78.

Karayolu Haber, 2013. http://karayoluhaber.com/2013/mus-bingol-karayolu-coktu/ Jan. 21, 2014.

Haberler, 2014. http://www.haberler.com/beytussebap-ta-bozuk-yol-sorunu-ele-alindi-4396800-haberi/ Jan. 21, 2014.

Haciefendioglu, K., Kartal, M.E., Karaca, Z., 2013. The effect of seasonally frozen soil on stochastic response of elevated water tank under random excitation. Stoch. Env. Res. Risk A. 27, 807–818.

He, R., Jin, H., 2010. Permafrost and cold-region environmental problems of the oil product pipeline from Golmud to Lhasa on the Qinghai–Tibet Plateau and their mitigation. Cold Reg. Sci. Technol. 64 (3), 279–288.

Hong, S., Kim, Y., Bae, G., Lee, J., 2011. A study on the frost penetration depth using measured value from pavement in Korea. Proceedings of the 21st International Offshore and Polar Engineering Conference, Maui, Hawaii, June 19–24.

Isard, S.A., Schaetzl, R.J., 1995. Estimating soil temperatures and frost in the lake effect snowbelt region, Michigan, USA. Cold Reg. Sci. Technol. 23 (4), 317–332.

Isik, A., Iyisan, R., Cevikbilen, G., Bayin, A., 2013. Frost susceptibility of fine grained soils related to consistency limits. Proceedings, 2nd International Balkans Conference on Challenges of Civil Engineering, BCCCE, May 23–25. Epoka University, Tirana, Albania.

Iwataa, Y., Nemoto, M., Hasegawa, S., Yanai, Y., Kuwao, K., Hirota, T., 2011. Influence of rain, air temperature, and snow cover on subsequent spring-snowmelt infiltration into thin frozen soil layer in Northern Japan. J. Hydrol. 401, 165–176.

Iwataa, Y., Hirota, T., Suzuki, T., Kuwao, K., 2012. Comparison of soil and thaw depths measured using frost tubes and other methods. Cold Reg. Sci. Technol. 11, 111–117.

Johansson, T., 2009. Artificial Ground Freezing in Clayey Soil: Laboratory and Field Studies of Deformations during Thawing at the Bothnia Line. Ph.D. dissertation. Dept. of Civil Architectural Engineering, Royal Institute of Technology, Stockholm, Sweden.

Johnston, G.H., 1982. Design and performance of the Inuvik, N.W.T., airstrip. Proceedings, 4th Canadian Permafrost Conference. Engineering Applications in Permafrost Areas, pp. 577–585.

Jorgenson, M.T., Kreigh, R.A., 1988. A model for mapping permafrost distribution based on landscape component maps and climatic variable. In: Senneset, K. (Ed.), Proceedings of the Fifth International Conference on Permafrost 1. Tapir Publishers, Trondheim, Norway (176.182).

Kalkan, E., 2009. Effects of silica fume on the geotechnical properties of fine grained soils exposed to freeze and thaw. Cold Reg. Sci. Technol. 58, 130–135.

Kamiloglu, H.A., Yılmaz, F., Sadoglu, E., 2012. An experimental examination of some factors affecting frost heave under freezing–thawing cycles. Proceedings, 3rd International Conference on New Developments in Soil Mechanics and Geotechnical Engineering, June 28–30. Near East University, Nicosia, North Cyprus.

Karaca, Z., Oztank, N., Gokce, M.V., Elci, H., 2011. Effects of surface-finishing forms and cement-filling on porous dimension limestone deterioration in cold regions. Cold Reg. Sci. Technol. 68, 124–128.

Klene, A.E., Nelson, F.E., Shiklomanov, N.I., Hinkel, K.M., 2001. The N-factor in natural landscapes: variability of air and soil-surface temperatures, Kuraruk River Basin, Alaska, USA. Arct. Antarct. Alp. Res. 33 (2), 140–148.

Lunardini, V.J., 1978. Theory of n-factors and correlation of data. In Proc. 3rd Int. Conf. on Permafrost, Edmonton, Alberta. 1. National Research Council of Canada, Ottawa, pp. 41–46

Lunardini, V.J., 1985. Analytical methods for ground thermal regime calculations. In: Krzewinski, T.G., Tart Jr, R.G. (Eds.), In Thermal Design Considerations in Frozen Ground Engineering. ASCE, New York, pp. 204–257.

Lautala, P., Harris, D., Ahlborn, T., Alkire, B., Hodek, R., 2012. Synthesis of railroad engineering best practices in areas of deep seasonal frost and permafrost final report. Rail Transportation Program. Michigan Tech Transportation Institute, Michigan Technological University.

Li, R., Shi, H., Flerchinger, G.N., Akae, T., Wang, C., 2012. Simulation of freezing and thawing soils in Inner Mongolia Hetao Irrigation District, China. Geoderma 173–174.

Maccaferri Environmental Technology Engineering, 2012. The Reinforcement Practices of the Infrastructure and Superstructure on Road Construction: Problems and Solutions. Maccaferri Environmental Technology Engineering, New Dehli.

Massachusetts Institute of Technology Department of Civil and Sanitary Engineering, Soil Engineering Division (MIT), 1957a. Frost penetration in multilayer soil profiles. Technical Report. Under Contract with Arctic Construction and Frost Effects Laboratory, New England division, Boston, MA.

McRoberts, E.C., 1974. Ground thermal regime. Recent Advances in Permafrost Engineering: Lecture Notes and Reference List. Dept. of Civil Engineering, Univ. of Alberta, Edmonton, Alberta, Canada.

Miller, H., Cabral, C., Kestler, M., Berg, R., Eaton, R., 2012. Calibration of a freeze–thaw prediction model for spring load restriction timing in northern New England. Proceedings, Cold Regions Engineering 2012: Sustainable Infrastructure Development in a Changing Cold Environment. ASCE, Reston, VA, pp. 369–379.

Olgun, M., 2013. The effects and optimization of additives for expansive clays under freeze–thaw conditions. Cold Reg. Sci. Technol. 93, 36–46.

Oztas, T., Fayetorbay, F., 2003. Effect of freezing and thawing processes on soil aggregate stability. Catena 52, 1–8.

Qi, J., Yao, X., Yu, F., Liu, Y., 2012. Study on thaw consolidation of permafrost under roadway embankment. Cold Reg. Sci. Technol. 81, 48–54.

Republic of Turkey Ministry of Transport (RTMT), 2011. Transportation in Turkey. Country Report, General Directorate of Turkish Highways, Motorway Development Program of Turkey, Suceava, Romania.

Saglik, A., Gungor, A.G., 2000. The guide of flexible superstructure planning on the highway. Department of Technical Research, Ministry of Transport, Ankara (in Turkish).

Saltan, M., Ozgungordu, M., Ozen, F.S., 2012. An environmental method against icing for road pavements, I: A new icy abrasion material and analysis. Proceedings, SIRWEC, Helsinki, May 23-25.

Sensoy, S., Demircan, M., Ulupinar, Y., Balta, I., 2008. Climate of Turkey. Turkish State Meteorological Service, 401, Ankara, Turkey http://www.mgm.gov.tr/files/en-us/climateofturkey.pdf Jan. 20, 2014.

Schimek, M.A., 2011. Topoclimatic influences on active-layer thickness, Northern Alaska (Master thesis). University of Delaware, Delaware, United States.

Shoop, S., Kestler, M., Stark, J., Ryerson, C., Affleck, R., 2002. Rapid stabilization of thawing soils: field experience and application. J. Terrramech. 39 (4), 181–194.

Simonsen, E., Isacsson, U., 1999. Thaw weakening of pavement structures in cold regions. Cold Reg. Sci. Technol. 29, 135–151.

Simonsen, E., Isacsson, U., 2001. Soil behavior during freezing and thawing using variable and constant confining pressure triaxial tests. Can. Geotech. J. 38, 863–875.

Tan, X., Chen, W., Tian, H., Cao, J., 2011. Water flow and heat transport including ice/water phase change in porous media: Numerical simulation and application. Cold Reg. Sci. Technol. 68, 74–84.

Wen, Z., Sheng, Y., Ma, W., Wu, Q., Wang, D., Sun, Z., Li, G., 2010. Probabilistic analysis of the replacement thickness of the in-cuts roadbed in permafrost regions. Cold Reg. Sci. Technol. 64 (1), 57–67.

Xiang, X.H., Wu, X.L., Wang, C.H., Chen, X., Shao, Q.Q., 2013. Influences of climate variation on thawing–freezing processes in the northeast of three-rivers source region in China. Cold Reg. Sci. Technol. 86, 86–97.

Yarbasi, N., Kalkan, E., Akbulut, S., 2007. Modification of the geotechnical properties, as influenced by freeze–thaw, of granular soils with waste additives. Cold Reg. Sci. Technol. 48, 44–54.

Zaimoglu, A.S., 2010. Freezing–thawing behavior of fine-grained soils reinforced with polypropylene fibers. Cold Reg. Sci. Technol. 60 (1), 63–65.

Zhao, H.X., Wu, Z.Q., Li, Z.Y., 2012. Experimental study on frost heave of silty clay in seasonally frost soil regions. Procedia Eng. 28, 282–286.